



Reactions of $\text{H}^+(\text{pyridine})_m(\text{H}_2\text{O})_n$ and $\text{H}^+(\text{NH}_3)_1(\text{pyridine})_m(\text{H}_2\text{O})_n$ with NH_3 : experiments and kinetic modelling

M. J. Ryding¹, Å. M. Jonsson², A. S. Zatula³, P. U. Andersson¹, and E. Uggerud³

¹Department of Chemistry, Atmospheric Science, University of Gothenburg, 412 96 Göteborg, Sweden

²IVL Swedish Environmental Research Institute Ltd., P.O. Box 5302, 400 14 Göteborg, Sweden

³Mass Spectrometry Laboratory and Centre for Theoretical and Computational Chemistry, Department of Chemistry, University of Oslo, P.O. Box 1033 Blindern, 0315 Oslo, Norway

Correspondence to: P. U. Andersson (pan@chem.gu.se)

Received: 23 June 2011 – Published in Atmos. Chem. Phys. Discuss.: 1 September 2011

Revised: 5 February 2012 – Accepted: 19 February 2012 – Published: 16 March 2012

Abstract. Reactions between pyridine containing water cluster ions, $\text{H}^+(\text{pyridine})_1(\text{H}_2\text{O})_n$, $\text{H}^+(\text{pyridine})_2(\text{H}_2\text{O})_n$ and $\text{H}^+(\text{NH}_3)_1(\text{pyridine})_1(\text{H}_2\text{O})_n$ (n up to 15) with NH_3 have been studied experimentally using a quadrupole time-of-flight mass spectrometer. The product ions in the reaction between $\text{H}^+(\text{pyridine})_m(\text{H}_2\text{O})_n$ ($m = 1$ to 2) and NH_3 have been determined for the first time. It is found that the reaction mainly leads to cluster ions of the form $\text{H}^+(\text{NH}_3)_1(\text{pyridine})_m(\text{H}_2\text{O})_{n-x}$, with $x = 1$ or 2 depending on the initial size of the reacting cluster ion. For a given number of water molecules (from 5 to 15) in the cluster ion, rate coefficients are found to be slightly lower than those for protonated pure water clusters reacting with ammonia. The rate coefficients obtained from this study are used in a kinetic cluster ion model under tropospheric conditions. The disagreement between ambient ground level measurements and previous models are discussed in relation to the results from our model and future experimental directions are suggested.

1 Introduction

Atmospheric ions are initially formed by solar radiation, galactic cosmic rays and radioactive decay. The ions are found in the entire atmosphere, although the formation mechanisms vary with altitude, region and time of day. The main products of the ionisation of air are O_2^+ , N_2^+ and free electrons (Wayne, 2000). Attachment of neutral polar molecules to the ions leads to charged molecular clusters. Subsequent to cluster formation and growth, ion-ion recombination of pos-

itively and negatively charged cluster ions may occur. For small clusters, this is believed to be associated with extensive fragmentation; for large clusters coalescence may occur. These larger neutral clusters formed by the recombination are suggested to be large enough to continue to grow spontaneously into new aerosol particles by condensation (Yu and Turco 2000; Yu 2003).

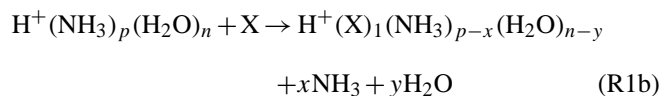
Several air ion mobility measurements have identified cluster ions in the troposphere. However, the chemical nature of these cluster ions is often difficult to identify (Horrak et al., 2000; Vana et al., 2008). By contrast, there have been measurements and identification of molecule ions in the troposphere during the last two decades. A large fraction of the molecule ions observed in these studies has likely originated from cluster ions that fragment before mass analysis (Eisele, 1983, 1986, 1988; Eisele and McDaniel, 1986; Eisele and Tanner, 1990; Schulte and Arnold, 1990). The first ground based measurement of atmospheric ion composition was performed by Perkins and Eisele in 1983 (Eisele, 1983; Perkins and Eisele, 1984). In the measurements, several unidentified positive ions were observed (Perkins and Eisele, 1984). Improved measurements conducted a few years later revealed the unidentified ions that had a mass-to-charge ratio of 80, 94 and 108 to be protonated pyridine ($\text{C}_5\text{H}_5\text{NH}^+$), protonated picoline (methyl-pyridine) and protonated lutidine (dimethyl-pyridine), respectively (Eisele, 1986, 1988). Several other ions have been identified in the troposphere in addition to these, although pyridinium and its derivatives are often found to dominate the mass spectrum. For example, Schulte and Arnold (1990) identified pyridinium as the dominating ion in air-plane based measurements in the free

troposphere over Europe. Recently, Junninen et al. (2010) measured day-time air ions at an urban site (the SMEAR III station in Helsinki), using an Atmospheric Pressure Interface Time-of-Flight instrument. They identified protonated poly(alkyl) pyridines as one of the main positive compound types. Ehn et al. (2010) measured day and night-time air ions at a remote site (the SMEAR II station in Hyytiälä) using the same instrument. They observed pyridine ions and alkyl substituted pyridine ions in both the day and night-time ion spectra, with approximately a factor two higher concentration during night-time.

Sources of atmospheric pyridine and pyridine derivatives are supposed to be biomass burning, automobile exhaust, coal tars and tobacco smoke (Clemo 1973; Saintjalm and Moreetesta, 1980; Beig, 2008). The main atmospheric sink is considered to be reaction with OH radicals (Eisele, 1986; Atkinson et al., 1987; Eisele, 1988; Yeung and Elrod, 2003). Yeung and Elrod (2003) calculated atmospheric lifetimes based on experimentally determined reaction rate coefficients for pyridine and for various substituted pyridine compounds to be 44 days and around 1 to 10 days, respectively. Other suggested atmospheric sinks of significance are reaction with HNO₃ in polluted environments (Atkinson et al., 1987) and reaction with atomic chlorine (Zhao et al., 2007). Due to the localised and sometimes irregular nature of the sources – as well as the relatively short atmospheric lifetimes – the concentration of pyridine is expected to be highly variable with time and location (Beig and Brasseur 2000; Yeung and Elrod, 2003). Few measurements of pyridine concentrations in the atmosphere exist. Among these, Tanner and Eisele (1991) measured a concentration of about 2.5 ppt ± 50 % ($6.2 \times 10^7 \text{ cm}^{-3}$) of molecular pyridine at Mauna Loa Observatory, Hawaii. In the measurements by Junninen et al. (2010) about 1 cm^{-3} of protonated pyridine was observed at the urban SMEAR III station in Helsinki. However, in contrast to most previous measurements they found up to six times higher concentrations for ionic alkyl substituted pyridine compounds $\text{H}^+\text{C}_5\text{H}_5\text{N}(\text{CH}_2)_n$, $1 \leq n \leq 6$, including picoline and lutidine. The reason for this is unknown but interesting and the findings show that there is a need to better understand the atmospheric chemistry of these compounds. Ehn et al. (2010) reported average concentrations of pyridinium and alkyl substituted pyridine ions from the SMEAR II station in Hyytiälä during 4 days in early May 2009: pyridinium 36.4 cm^{-3} , picolinium 57.3 cm^{-3} , lutidinium 33.5 cm^{-3} . Also in this case, alkyl substituted pyridine ions were higher in concentration than the pyridine ion.

A kinetic cluster ion model by Beig and Brasseur (2000) indicate that pyridine-containing clusters may be the dominating positive ions in the lower free troposphere (from 1 to 6 km above ground). More specifically, the pyridinated cluster ions in the model were $\text{H}^+(\text{X})_1(\text{H}_2\text{O})_n$ and $\text{H}^+(\text{NH}_3)_p(\text{X})_1(\text{H}_2\text{O})_n$, where X = pyridine, picoline or lutidine. Beig and Brasseur proposed two reaction pathways

for the formation of these pyridinated cluster ions from $\text{H}^+(\text{H}_2\text{O})_n$ clusters. The first reaction pathway starts with addition of NH₃ to a protonated water cluster. The formed cluster can thereafter react with a pyridine type molecule X:



In the second reaction pathway, a pyridine molecule reacts with a protonated water cluster. The pyridine is thereafter ejected when ammonia attaches to the cluster in a second step:



The second step can thereafter be followed by Reaction (R1b) above to form a cluster containing both ammonia and pyridine. The driving force behind these reactions – forming cluster ions containing ammonia and pyridine derivatives – appears connected to the high basicities of ammonia and the pyridine derivatives. Note that loss of water is likely to occur also in the first step of the first mechanism (Reaction R1a) and in the second step of the second mechanism (Reaction R2b); however, this was not included in the notation by Beig and Brasseur.

The rate coefficients for the first three reactions have been determined by Viggiano et al. for the case X = pyridine (Viggiano et al., 1988a, b). The rate coefficients were found to be approximately equal to the collision rate constant. The rate of Reaction (R2b) is unknown; Beig and Brasseur assumed $10^{-11} \text{ cm}^{-3} \text{ s}^{-1}$ as an upper limit for the rate coefficient for all pyridine derivatives in their study, this is two orders of magnitude lower than the rate coefficient for Reaction (R1b) at 298 K.

The pyridinated cluster ions, $\text{H}^+(\text{X})_1(\text{NH}_3)_p(\text{H}_2\text{O})_n$, which may be the dominating positive cluster ions in the atmosphere, as suggested by Beig and Brasseur, could potentially be an important source for new aerosol formation. However, these cluster ions have to date not been measured in the atmosphere. This discrepancy has motivated us to perform well controlled experiments to investigate the formation mechanisms of these clusters. The reactions of two types of cluster ions with NH₃ in a cluster beam experiment are studied; the clusters being $\text{H}^+(\text{pyridine})_m(\text{H}_2\text{O})_n$ ($m = 1$ to 2 , $n \leq 15$) and $\text{H}^+(\text{NH}_3)_1(\text{pyridine})_1(\text{H}_2\text{O})_n$ (also $n \leq 15$). The results from the experiments are input to improve the present kinetic model by Beig and Brasseur for atmospheric positive ions. The importance of evaporation of pyridine from the cluster ions is also studied in the improved model. Finally, the atmospheric implications of the experimental results and the results from the kinetic modelling are discussed.

2 Methods

2.1 Experimental

The experiments were performed using a modified quadrupole time-of-flight mass spectrometer (QTOF 2, Micromass/Waters, Manchester UK). The instrument and experimental procedure has been described in detail previously (Andersson et al., 2008; Ryding et al., 2011), and therefore only a brief overview is presented here. The cluster ions were produced from aqueous solutions at atmospheric pressure by electrospray ionization (ESI) and thereafter entered into the high vacuum part of the instrument. Two different solutions were used: 2.5 mM pyridine(aq) for production of $\text{H}^+(\text{pyridine})_m(\text{H}_2\text{O})_n$ ($m = 1$ to 2, $n \leq 15$) ions and a mixture with 2.5 mM pyridine(aq) and 30 mM NH_3 (aq) for production of $\text{H}^+(\text{NH}_3)_1(\text{pyridine})_1(\text{H}_2\text{O})_n$ ions. A quadrupole mass filter (with better than unit resolution) allowed for selection of single sized clusters based on their mass-to-charge ratio, m/z . The selected clusters then entered the collision cell, where they were brought to collide with gaseous ammonia at a centre-of-mass (COM) collision energy $E_{\text{COM}} = 8 \text{ kJ mol}^{-1}$ (0.085 eV). The resulting products were analyzed by a reflectron time-of-flight (TOF) mass analyzer set at a mass resolution, $m/\Delta m$, of about 5000 (full-width-half-height). The ammonia was introduced into the collision cell through an Ultra-High-Vacuum (UHV) leak valve giving a pressure of about 10^{-5} mbar. This pressure of NH_3 was chosen to keep the number of collisions below 10% to ensure single-collision conditions for the entire range of cluster sizes. Reference measurements were collected by measuring the cluster ion $\text{H}^+(\text{pyridine})_1(\text{H}_2\text{O})_{11}$ at regular intervals during the experiment to make sure that the collision gas pressure was constant. For each measurement, a corresponding background measurement was collected with an empty collision cell. Due to limitations with the current setup the instrument is unable to accurately measure ions below $m/z = 50$; for this reason, the lightest cluster investigated was $\text{H}^+(\text{H}_2\text{O})_4$. For the cluster ions $\text{H}^+(\text{pyridine})_1(\text{H}_2\text{O})_{10}$ and $\text{H}^+(\text{NH}_3)_1(\text{pyridine})_1(\text{H}_2\text{O})_{10}$ measurements were also performed at various collision energies between 1.45 kJ mol^{-1} and 120 kJ mol^{-1} (COM). A separate set of measurements were performed in order to estimate the evaporation of pyridine from clusters: $\text{H}^+(\text{pyridine})_m(\text{H}_2\text{O})_5$ and $\text{H}^+(\text{NH}_3)_1(\text{pyridine})_m(\text{H}_2\text{O})_5$ with $m = 1$ to 4 was allowed to pass through the empty collision cell at varying collision energies. In the first series, the energies varied from 0.4 to 2.0 eV (in the lab frame) corresponding to 39 to 193 kJ mol^{-1} , in the second series the energies varied from 0.1 to 0.7 eV corresponding to 10 to 68 kJ mol^{-1} . For producing the clusters containing three or four pyridine molecules, the pyridine concentration in the aqueous solutions was increased to 1.5 M. Reagents used in the experiments: H_2O (no. 95270 for HPLC, Fluka),

pyridine (99.5%, BDH Chemicals Ltd.), NH_3 (99.96%, AGA), 25% NH_3 (aq) (Pro analysi, Merck).

2.2 Positive ion model description

The positive cluster ion reaction schemes in this paper are based on the aforementioned model by Beig and Brasseur (2000). In their model, protonated water clusters, $\text{H}^+(\text{H}_2\text{O})_n$, are continuously produced in a series of reactions starting from O_2^+ and N_2^+ . Initially, ions O_2^+ and N_2^+ are formed by galactic cosmic rays and by radioactive decay (close to ground). Charge transfer reactions with molecular oxygen convert N_2^+ to O_2^+ . The latter ion then forms O_4^+ , which in turn reacts with H_2O to form $\text{O}_2^+(\text{H}_2\text{O})$. Additional H_2O molecules add to the cluster, which forms $\text{H}^+(\text{H}_2\text{O})_n$ via loss of O_2 and OH (Beig et al., 1993). Subsequent to this, the protonated water clusters may then react with ammonia, pyridine, picoline, lutidine, acetone and acetonitrile. The production of cluster ions is balanced by the loss of cluster ions through ion-ion recombination and attachment to aerosol particles. The concentration of negative ions in the model was set equal to the concentration of positive ions. In our first model (Model A), we have made two modifications to the model by Beig and Brasseur. Firstly, we have included the experimental results from this study. That is, in the reaction between $\text{H}^+(\text{pyridine})_m(\text{H}_2\text{O})_n$ ($m = 1$ to 2, $n \leq 15$) and NH_3 virtually no exchange of pyridine for ammonia will take place. Instead, ammonia is incorporated into the cluster ion with subsequent loss of one or two water molecules, i.e. $\text{H}^+(\text{pyridine})_m(\text{H}_2\text{O})_n + \text{NH}_3 \rightarrow \text{H}^+(\text{NH}_3)_1(\text{pyridine})_m(\text{H}_2\text{O})_{n-x} + x\text{H}_2\text{O}$. Hence, the former reaction was excluded from the model and the latter was added (the corresponding modifications were made for the reactions with clusters containing picoline and lutidine). For simplicity, the rate coefficient for $\text{H}^+(\text{pyridine})_1(\text{H}_2\text{O})_4 + \text{NH}_3$ (obtained in this study) was used for all pyridine/water clusters. Secondly, we have included reactions leading to clusters containing two amines (pyridine, picoline and lutidine). The reactions included in Model A are shown in Fig. 1 and the corresponding rate coefficients are given in Table 1. In our second model, Model B, we have omitted the amines picoline and lutidine since pyridine-containing cluster ions are found to be the dominating cluster ions in Model A. We also allowed for up to five pyridine molecules in each cluster. In this model we regard pyridine as a representative for all amines as most amines have high proton affinities and many other amine ions have been found in the atmosphere. The reactions included in this model are shown in Fig. 2 and the corresponding rate coefficients are given in Table 1. In the absence of detailed data for evaporation of pyridine from protonated water clusters and since we do not observe evaporation of pyridine under our experimental conditions (see Sect. 3.1), we excluded evaporation of pyridine in most of the model studies presented in this study. The differential rate equations were solved

Table 1. Rate coefficients for the reactions used in Model A and Model B.

Reaction	Rate coefficient, cm ³ s ⁻¹	Reference
Formation of H ⁺ (H ₂ O) _n	$Rate_1 = 2$ (unit: cm ⁻³ s ⁻¹)	Beig and Brasseur (2000) ^a
H ⁺ (H ₂ O) _n + qCH ₃ CN → H ⁺ (CH ₃ CN) _q (H ₂ O) _n	$k_1 = 3.06 \times 10^{-9}(300/T)$	Viggiano et al. (1988a)
H ⁺ (H ₂ O) _n + pNH ₃ → H ⁺ (NH ₃) _p (H ₂ O) _n	$k_2 = 1.91 \times 10^{-9}(300/T)^{0.39}$	Viggiano et al. (1988a)
H ⁺ (H ₂ O) _n + CH ₃ COCH ₃ → H ⁺ (CH ₃ COCH ₃) ₁ (H ₂ O) _n	$k_3 = 2.04 \times 10^{-9}(300/T)^{0.59}$	Viggiano et al. (1988a)
H ⁺ (CH ₃ COCH ₃) ₁ (H ₂ O) _n + pNH ₃ → H ⁺ (NH ₃) _p (H ₂ O) _n	$k_4 = 2 \times 10^{-9}$	Hauck and Arnold (1984)
H ⁺ (CH ₃ CN) _q (H ₂ O) _n + CH ₃ COCH ₃ → H ⁺ (CH ₃ COCH ₃) ₁ (H ₂ O) _n	$k_5 = 1.8 \times 10^{-9}$	Hauck and Arnold (1984)
H ⁺ (CH ₃ CN) _q (H ₂ O) _n + pNH ₃ → H ⁺ (NH ₃) _p (H ₂ O) _n	$k_6 = 1.8 \times 10^{-9}$	Schlager et al. (1983)
H ⁺ (NH ₃) _p (H ₂ O) _n + picoline → H ⁺ (NH ₃) _p (picoline) ₁ (H ₂ O) _n	$k_7 = 2.6 \times 10^{-9}(300/T)^{0.7}$	Viggiano et al. (1988b)
H ⁺ (NH ₃) _p (H ₂ O) _n + lutidine → H ⁺ (NH ₃) _p (lutidine) ₁ (H ₂ O) _n	$k_8 = 2 \times 10^{-9}$	assumed ^b
H ⁺ (NH ₃) _p (H ₂ O) _n + pyridine → H ⁺ (NH ₃) _p (pyridine) ₁ (H ₂ O) _n	$k_9 = 2.1 \times 10^{-9}(300/T)^{0.7}$	Viggiano et al. (1988b)
H ⁺ (H ₂ O) _n + picoline → H ⁺ (picoline) ₁ (H ₂ O) _n	$k_{10} = 2 \times 10^{-9}$	assumed ^b
H ⁺ (H ₂ O) _n + lutidine → H ⁺ (lutidine) ₁ (H ₂ O) _n	$k_{11} = 2 \times 10^{-9}$	assumed ^b
H ⁺ (H ₂ O) _n + pyridine → H ⁺ (pyridine) ₁ (H ₂ O) _n	$k_{12} = 2.08 \times 10^{-9}(300/T)^{0.89}$	Viggiano et al. (1988a)
H ⁺ (X) ₁ (H ₂ O) _n + pNH ₃ → H ⁺ (NH ₃) _p (X) ₁ (H ₂ O) _n	$k_{13} = k_{14} = k_{15} = 0^c$	assumed
cluster + aerosol → aerosol ion	$k_{16} = 5 \times 10^{-6}$	Beig and Brasseur (2000)
cluster + cluster recombination	$k_{17} = 6 \times 10^{-8}(300/T)^{0.5}$ $+ 1.25 \times 10^{-25}[M](300/T)^4^d$	Arijs and Brasseur (1986), Beig et al. (1993)
H ⁺ (X) ₁ (H ₂ O) _n + pNH ₃ → H ⁺ (NH ₃) _p (X) ₁ (H ₂ O) _n	$k_{18} = 0.907 \times k_2$	this work
H ⁺ (X) ₁ (H ₂ O) _n + X → H ⁺ (X) ₂ (H ₂ O) _n	$k_{19} = k_{12}$	assumed
H ⁺ (NH ₃) _p (X) ₁ (H ₂ O) _n + pyridine → H ⁺ (NH ₃) _p (X) ₂ (H ₂ O) _n	$k_{20} = k_9$	assumed
H ⁺ (NH ₃) _p (X) ₁ (H ₂ O) _n + picoline → H ⁺ (NH ₃) _p (X) ₂ (H ₂ O) _n	$k_{21} = k_7$	assumed
H ⁺ (NH ₃) _p (X) ₁ (H ₂ O) _n + lutidine → H ⁺ (NH ₃) _p (X) ₂ (H ₂ O) _n	$k_{22} = k_8$	assumed
H ⁺ (X) ₂ (H ₂ O) _n + pNH ₃ → H ⁺ (NH ₃) _p (X) ₂ (H ₂ O) _n	$k_{23} = k_{18}$	assumed
H ⁺ (NH ₃) _p (X) ₂ (H ₂ O) _n + pyridine → H ⁺ (NH ₃) _p (X) ₃ (H ₂ O) _n	$k_{24} = k_9$	assumed
H ⁺ (NH ₃) _p (X) ₃ (H ₂ O) _n + pyridine → H ⁺ (NH ₃) _p (X) ₄ (H ₂ O) _n	$k_{25} = k_9$	assumed
H ⁺ (NH ₃) _p (X) ₄ (H ₂ O) _n + pyridine → H ⁺ (NH ₃) _p (X) ₅ (H ₂ O) _n	$k_{26} = k_9$	assumed

Note that X = pyridine, picoline or lutidine.

^a The formation of H⁺(H₂O)_n was set to give the same rate as used by Beig and Brasseur (2000).

^b The value is the same as used by Beig and Brasseur (2000).

^c A value of 1×10^{-11} cm⁻³ s⁻¹ was used by Beig and Brasseur (2000).

^d [M] is the neutral number density in cm⁻³.

for H⁺(pyridine)₁(H₂O)₁₁, with the notable exception that loss of a single pyridine molecule (m/z 79 u smaller than the parent ion) and loss of a pyridine molecule accompanied by loss of a water molecule (m/z 97 u smaller than the parent ion) can be observed. The peaks are found with approximately the same intensity in the background measurement and in the measurement with NH₃ present in the collision cell, with somewhat higher abundance in the former case. However, as will be discussed later, this loss of pyridine is likely resulting from collision induced dissociation (CID) and not evaporation. Due to the above mentioned evaporation of H₂O molecules from the parent ion, some of the detected products will have originated from reactions of pre-formed evaporation products. In order to estimate the contribution of these reactions, we devised the following simple model. The peak at m/z 1 u smaller than the parent ion represents the reaction $A^+(H_2O)_n + NH_3 \rightarrow A^+(NH_3)_1(H_2O)_{n-1} + H_2O$ (with $A^+ = H^+$, H⁺(pyridine)₁, H⁺(pyridine)₂ or H⁺(NH₃)₁(pyridine)₁). We assume

that all of the evaporation products $A^+(H_2O)_{n-x}$, $x = 1, 2, 3$ in a mass spectrum would form the products $A^+(NH_3)_1(H_2O)_{n-x-1}$, $x = 1, 2, 3$ to a degree that corresponds to the relative intensity of the peak 1 u smaller than the parent ion in a mass spectrum where $A^+(H_2O)_{n-x}$, $x = 1, 2, 3$ is the parent ion. This gives a small contribution from the $A^+(H_2O)_{n-1}$ cluster to the $A^+(NH_3)_1(H_2O)_{n-2}$ peak, located at m/z 19 u smaller than the parent ion. The remaining intensity in this peak originate from the parent ion reaction $A^+(H_2O)_n + NH_3 \rightarrow A^+(NH_3)_1(H_2O)_{n-2} + 2H_2O$. We calculated the magnitude of this reaction for all parent ion cluster sizes, and applied it to the correspondingly sized evaporation products as well. We were then able to estimate the magnitude of the third parent ion reaction: $A^+(H_2O)_n + NH_3 \rightarrow A^+(NH_3)_1(H_2O)_{n-3} + 3H_2O$ in the same way. A more thorough description of the procedure can be found in the Supplement.

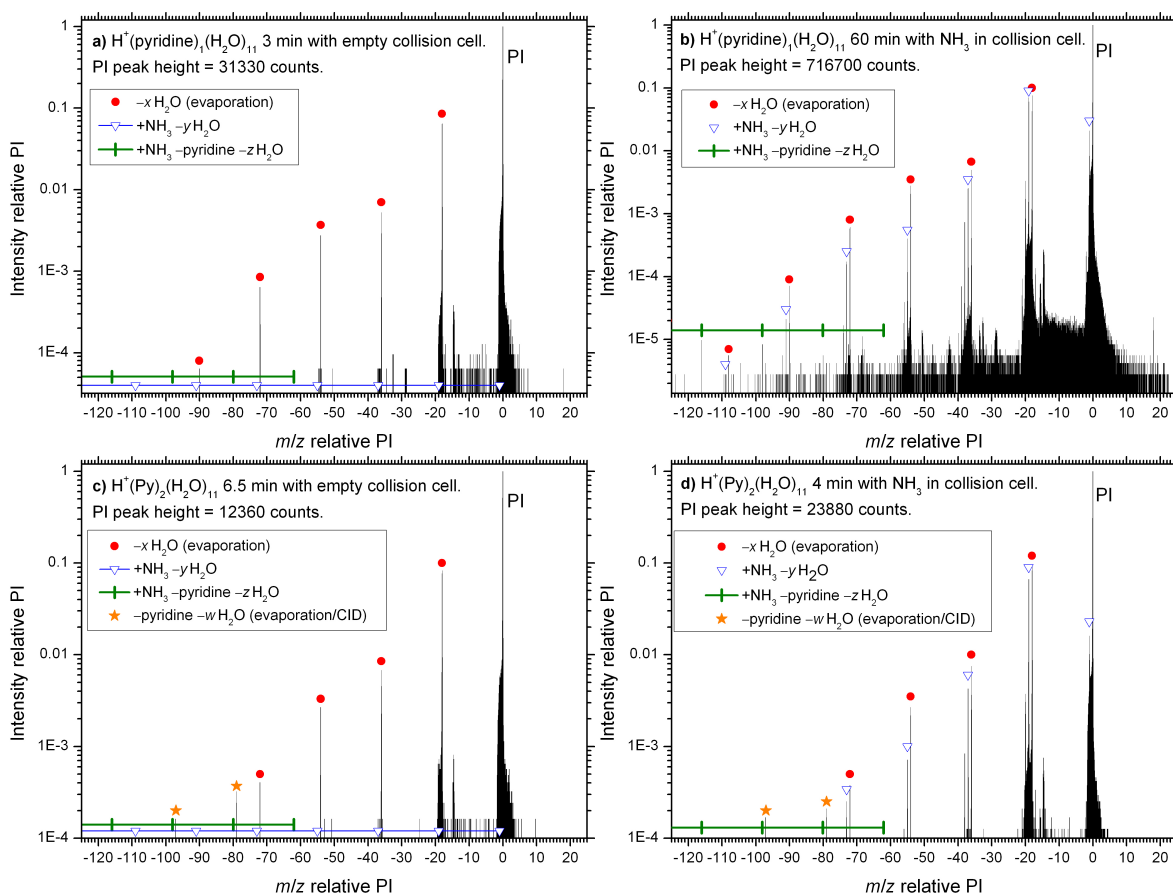


Fig. 3. Mass spectra of $\text{H}^+(\text{pyridine})_m(\text{H}_2\text{O})_{11}$ with peak intensities expressed relative to the parent ion (PI) mass and height. (a) $m = 1$, background measurement. (b) $m = 1$, the cluster ion reacting with NH_3 at 8 kJ mol^{-1} . (c) $m = 2$, background measurement. (d) $m = 2$, the cluster ion reacting with NH_3 at 8 kJ mol^{-1} . The product $\text{H}^+(\text{NH}_3)_1(\text{pyridine})_1(\text{H}_2\text{O})_{11-y}$ peaks are designated by open blue triangles. Red circles designate peaks arising from evaporation of H_2O from the parent ion. Green vertical lines designate the m/z where a possible $\text{NH}_3/\text{pyridine}$ exchange product, $\text{H}^+(\text{NH}_3)_1(\text{H}_2\text{O})_{10-z}$, would appear. Loss of pyridine without exchange for NH_3 is designated by orange stars.

Figure 4 shows the branching ratios of different products from the $\text{H}^+(\text{pyridine})_m(\text{H}_2\text{O})_n + \text{NH}_3$ reaction ($m = 0$ to 2) at $E_{\text{COM}} = 8 \text{ kJ mol}^{-1}$. For $\text{H}^+(\text{H}_2\text{O})_n + \text{NH}_3$ the main product peaks represent incorporation of the NH_3 molecule and loss of two or three water molecules. The simple model described above attributes the intensity of these peaks to reactions of the parent ion (by 100 % and ≥ 90 %, respectively). Peaks corresponding to addition of the ammonia molecule and loss of four and five H_2O from the parent cluster can be seen; they tend to be higher for the larger clusters. A significant part of the abundance of these products is likely resulting from reactions of evaporation products; they have been included for comparison. Loss of a single water molecule after reaction with NH_3 is effectively not observed for this cluster type.

The branching ratios of the $\text{H}^+(\text{pyridine})_1(\text{H}_2\text{O})_n$ and $\text{H}^+(\text{pyridine})_2(\text{H}_2\text{O})_n$ clusters are rather similar, and are dominated by loss of two water molecules after addition of the ammonia molecule. For smaller clusters, loss of a single water molecule occurs with a frequency similar to the loss of two water molecules. However, the $-\text{H}_2\text{O}$ curve drops off with size, giving about an order of magnitude lower abundance compared to the $-2\text{H}_2\text{O}$ products as n approaches 15. Both of these peaks are due to parent ion reactions, while the peaks corresponding to loss of three or four water molecules after addition of ammonia is likely to contain large contributions from reactions of evaporation clusters. Again, we notice that virtually no pyridine leaves the cluster ions after reaction with ammonia, neither for $\text{H}^+(\text{pyridine})_1(\text{H}_2\text{O})_n$ nor for $\text{H}^+(\text{pyridine})_2(\text{H}_2\text{O})_n$. This is in contrast to the assumption made by Beig and Brasseur (2000).

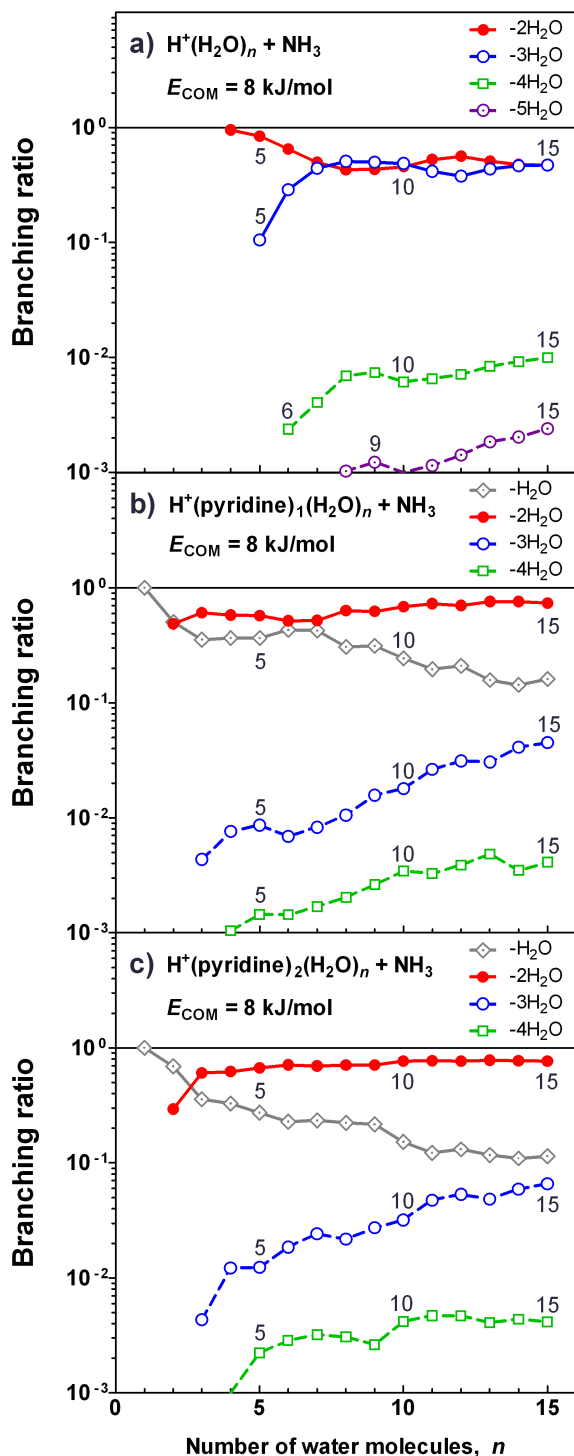


Fig. 4. Branching ratios for the reactions of $\text{H}^+(\text{pyridine})_m(\text{H}_2\text{O})_n$ ($m = 0$ to 2) with NH_3 at $E_{\text{COM}} = 8 \text{ kJ mol}^{-1}$. The number of water molecules, n , is indicated for some of the data points to improve readability. Dashed lines indicate products likely resulting from clusters that have lost water molecules prior to reaction.

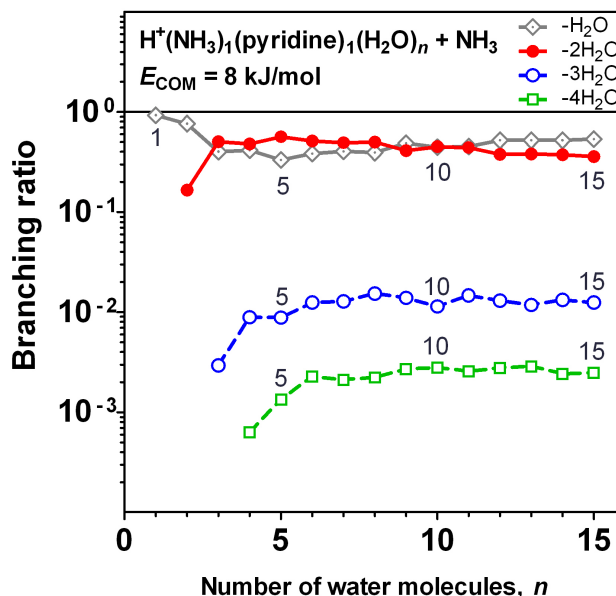


Fig. 5. Branching ratios for $\text{H}^+(\text{NH}_3)_1(\text{pyridine})_1(\text{H}_2\text{O})_n$ reacting with NH_3 at $E_{\text{COM}} = 8 \text{ kJ mol}^{-1}$. The curves represent peaks corresponding to the parent ion incorporating NH_3 and losing one to four H_2O . Dashed lines indicate products likely resulting from clusters that have lost water molecules prior to reaction. The numbers next to the curves indicate the number of water molecules, n .

Branching ratios for the $\text{H}^+(\text{NH}_3)_1(\text{pyridine})_1(\text{H}_2\text{O})_n + \text{NH}_3$ reaction are shown in Fig. 5 for $n = 1$ to 15 . As seen, the products are dominated by incorporation of the reactant NH_3 and loss of one or two water molecules in more or less equal amounts, except for $n = 2$. Again, these reactions can be attributed to the parent ion by 100 % and ≥ 90 %, respectively. Products with three or four water molecules fewer than the parent ion are also observed and are likely formed from evaporation product reactions. Common for all the curves in Fig. 5 is that they show less size dependence than the clusters in Fig. 4.

The reaction rate coefficients for the clusters $\text{H}^+(\text{H}_2\text{O})_n$, $\text{H}^+(\text{pyridine})_1(\text{H}_2\text{O})_n$, $\text{H}^+(\text{pyridine})_2(\text{H}_2\text{O})_n$ and $\text{H}^+(\text{NH}_3)_1(\text{pyridine})_1(\text{H}_2\text{O})_n$ reacting with NH_3 at 8 kJ mol^{-1} (COM) are found in Fig. 6 as a function of the number of water molecules in the cluster, $n = 1$ to 15 ($n = 4$ to 15 in the case of pure water clusters). In the absence of an exactly calibrated NH_3 pressure in the collision cell the reaction rate coefficients are expressed relative to the rate coefficient of the $\text{H}^+(\text{H}_2\text{O})_4$ cluster. It should, however, be mentioned that reference measurements show the pressure to be constant during the course of the experiments. The thermal rate coefficients for the reference cluster $\text{H}^+(\text{H}_2\text{O})_4$ is $1.91 \times 10^{-9} (300/T)^{0.39} \text{ cm}^3 \text{ s}^{-1}$, (Viggiano et al., 1988a). For the same cluster reacting with ND_3 at $E_{\text{COM}} = 8 \text{ kJ mol}^{-1}$ (0.085 eV) Honma et al. (1992) reported a reaction cross section of approximately $1.5 \times 10^{-14} \text{ cm}^2$.

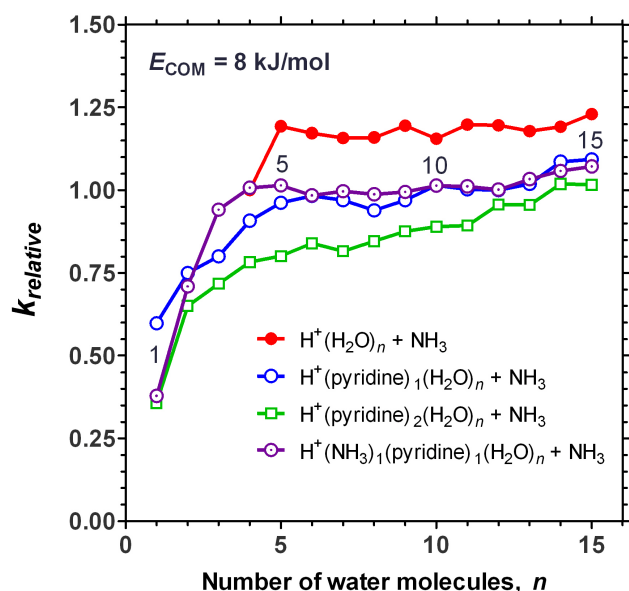


Fig. 6. Relative reaction rate coefficients for cluster ions $\text{H}^+(\text{pyridine})_m(\text{H}_2\text{O})_n$ (with $m = 0$ to 2) and $\text{H}^+(\text{NH}_3)_1(\text{pyridine})_1(\text{H}_2\text{O})_n$, reacting with NH_3 at $E_{\text{COM}} = 8 \text{ kJ mol}^{-1}$. The rate coefficients are normalized to the rate coefficient for $\text{H}^+(\text{H}_2\text{O})_4$ reacting with NH_3 ($1.91 \times 10^{-9} \text{ cm}^3 \text{ s}^{-1}$ at 298 K (Viggiano et al., 1988a)). The numbers 1, 5, 10, 15 indicate the number of water molecules to improve readability.

For the present case, given a velocity of 1090 ms^{-1} through the collision cell, this corresponds to a reaction rate coefficient of $1.6 \times 10^{-9} \text{ cm}^3 \text{ s}^{-1}$ for the reference cluster. As can be seen in Fig. 6, pure water clusters exhibit a somewhat higher reaction rate in the size range $n = 5$ to 15 compared to the pyridine containing clusters.

In order to estimate the rate coefficient for exchanging a pyridine molecule in a cluster with an ammonia molecule i.e. Reaction (R2b) above, we calculated the total abundance of the peaks corresponding to incorporation of ammonia and loss of pyridine and 0 to 2 water molecules. We found that for $\text{H}^+(\text{pyridine})_m(\text{H}_2\text{O})_n$ clusters with $m = 1$ to 2 and $n = 1$ to 15, the maximum relative rate coefficient for loss of pyridine was 8.0×10^{-4} (the standard deviation due to signal statistics is 2.4×10^{-4}) relative the total rate coefficient for $\text{H}^+(\text{H}_2\text{O})_4 + \text{NH}_3$. Using the value by Viggiano et al. (1988a) for the latter, this gives a rate coefficient of $1.5 \times 10^{-12} \text{ cm}^3 \text{ s}^{-1}$ (at 298 K) for the reaction $\text{H}^+(\text{pyridine})_1(\text{H}_2\text{O})_n + \text{NH}_3 \rightarrow \text{H}^+(\text{NH}_3)_1(\text{H}_2\text{O})_{n-x} + x\text{H}_2\text{O} + \text{pyridine}$. This is a factor of 7 lower than $1 \times 10^{-11} \text{ cm}^3 \text{ s}^{-1}$ as assumed by Beig and Brasseur. However, for the majority of the clusters in our study the reaction rate coefficient is even lower. Typical values of the rate coefficient for the above reaction is in the range of 1×10^{-4} to 4×10^{-4} relative $\text{H}^+(\text{H}_2\text{O})_4$.

Table 2. Initial concentrations in cm^{-3} for the simulations presented in Figs. 7 and 8.

Figure	7	8a–b	8c–d
Model	A	B	B
NH_3	2.46×10^{10}	2.46×10^{10}	4.92×10^8
H_2O	4.61×10^{17}	4.61×10^{17}	4.61×10^{17}
Pyridine	variable	variable	variable
Picoline	[pyridine]/10	–	–
Lutidine	[pyridine]/10	–	–
Acetone	3.69×10^{10}	3.69×10^{10}	3.69×10^{10}
CH_3CN	4.92×10^8	4.92×10^8	4.92×10^8
Aerosol	1.0×10^3	1.0×10^3	1.0×10^3
Negative ions	= [positive ions]	= [positive ions]	= [positive ions]

Separate measurements were performed in order to estimate the evaporation of pyridine from clusters containing between one and four pyridine molecules and up to one ammonia molecule. In the Supplement these measurements are described. To summarise, we were unable to determine the evaporation rate coefficients for loss of pyridine from neither of the clusters since a potential weak signal from evaporation could not be separated from collision induced dissociation losses. However, we conclude that the evaporation rate coefficient is of the order 0.1 s^{-1} or lower under the experimental conditions.

3.2 Modelling results

We have modelled the reaction kinetics using three different models. First we performed a calculation using the model of Beig and Brasseur applying their set of parameters, and successfully reproduced their results. We thereafter used Model A at different pyridine concentrations. The concentrations used for all molecules in the model are shown in Table 2. The results are shown in Fig. 7 on a linear scale (in the Supplement the results are shown on a logarithmic scale to include also ions with low concentrations). At pyridine concentrations below 10^4 cm^{-3} , clusters of the type $\text{H}^+(\text{NH}_3)_p(\text{H}_2\text{O})_n$ dominate completely but already at pyridine concentrations of $2.8 \times 10^6 \text{ cm}^{-3}$, 50% of the clusters contain both pyridine and ammonia. At concentrations above $5 \times 10^6 \text{ cm}^{-3}$, clusters with ammonia, water and two pyridine molecules dominate. Since the lutidine and picoline concentration is 10 times lower than the pyridine concentration, clusters containing both pyridine and lutidine or picoline are found in concentrations about 10 times lower than the concentration of $\text{H}^+(\text{NH}_3)_p(\text{pyridine})_2(\text{H}_2\text{O})_n$. In order to evaluate the importance of including the reaction $\text{H}^+(\text{pyridine})_1(\text{H}_2\text{O})_n + p\text{NH}_3 \rightarrow \text{H}^+(\text{NH}_3)_p(\text{pyridine})_1(\text{H}_2\text{O})_{n-x} + x\text{H}_2\text{O}$ in Model A, we also performed calculations in which we substituted this reaction with $\text{H}^+(\text{pyridine})_1(\text{H}_2\text{O})_n + p\text{NH}_3 \rightarrow \text{H}^+(\text{NH}_3)_p(\text{H}_2\text{O})_{n-x} + x\text{H}_2\text{O} + \text{pyridine}$, i.e.

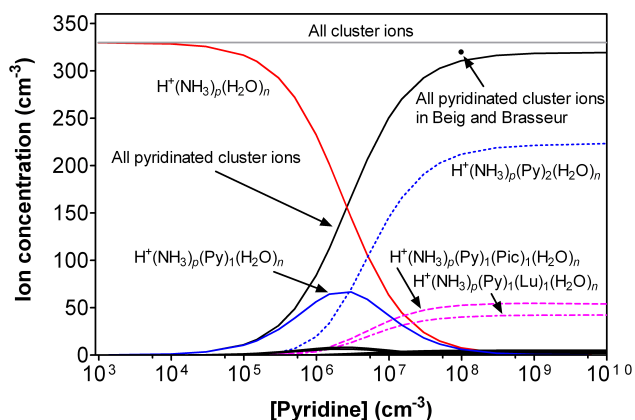


Fig. 7. Concentration of cluster ions as a function of pyridine concentration. The values were calculated using Model A and the initial concentrations are given in Table 2. The total concentration of pyridinated cluster ions in the model by Beig and Brasseur (2000) is also indicated. Py, Pic and Lu indicate pyridine, picoline and lutidine, respectively.

Reaction (R2b). Essentially no difference in ion concentrations obtained from the two models were observed, neither at an ammonia concentration of $2.46 \times 10^{10} \text{ cm}^{-3}$ nor at an ammonia concentration 50 times lower.

A typical pyridine concentration in the troposphere is around 4 ppt ($9.9 \times 10^7 \text{ cm}^{-3}$ at 298 K) (Eisele, 1988; Tanner and Eisele, 1991). From Fig. 7 it is clear that more than one pyridine molecule may be present in the cluster ions in the atmosphere provided that evaporation of pyridine from the cluster is small compared to the formation mechanisms (as assumed in the model). In order to study this in more detail we constructed Model B, where up to five pyridine molecules are allowed to be incorporated in each cluster. In Fig. 8, we show the ion concentration as a function of pyridine concentration at a typical ammonia concentration (1.0 ppb , or $2.46 \times 10^{10} \text{ cm}^{-3}$). Assuming no evaporation, a pyridine concentration of 4 ppt ($9.9 \times 10^7 \text{ cm}^{-3}$) would give more than four pyridine molecules in most clusters (the maximum number of pyridine molecules in a cluster is five in the model, but the number of pyridine molecules in such a cluster should be regarded as five or more). Neglecting evaporation of pyridine may not be realistic, but this model shows that clusters with a multiple number of pyridine molecules may be present in the atmosphere if evaporation is low (the influence of the evaporation rate on the number of pyridine molecules in the cluster is presented below). In Fig. 8b, the concentrations from Fig. 8a are shown on a logarithmic scale. The concentration of $\text{H}^+(\text{CH}_3\text{COCH}_3)_1(\text{H}_2\text{O})_n$, $\text{H}^+(\text{H}_2\text{O})_n$, and $\text{H}^+(\text{CH}_3\text{CN})_q(\text{H}_2\text{O})_n$ are all below 0.1 cm^{-3} at all pyridine concentrations used. The concentration of $\text{H}^+(\text{pyridine})_m(\text{H}_2\text{O})_n$ $1 \leq m \leq 5$ are also well below 0.1 cm^{-3} at pyridine concentrations below $3 \times 10^{10} \text{ cm}^{-3}$ and an ammonia concentration of $2.46 \times 10^{10} \text{ cm}^{-3}$.

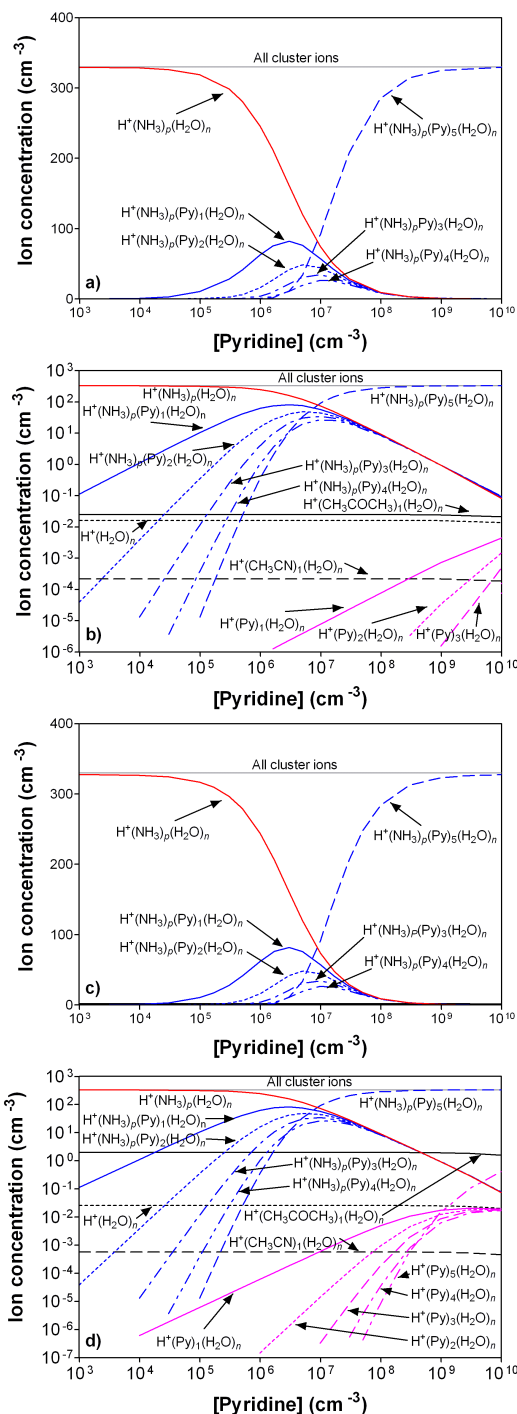


Fig. 8. Concentration of cluster ions as a function of pyridine concentration. The values were calculated using Model B and the initial concentrations are given in Table 2. Panel (a) and (b) shows the results using an ammonia concentration of $2.46 \times 10^{10} \text{ cm}^{-3}$ on a linear and logarithmic scale, respectively. Panel (c) and (d) shows the results for an ammonia concentration of $4.92 \times 10^8 \text{ cm}^{-3}$. Py, Pic and Lu indicate pyridine, picoline and lutidine, respectively.

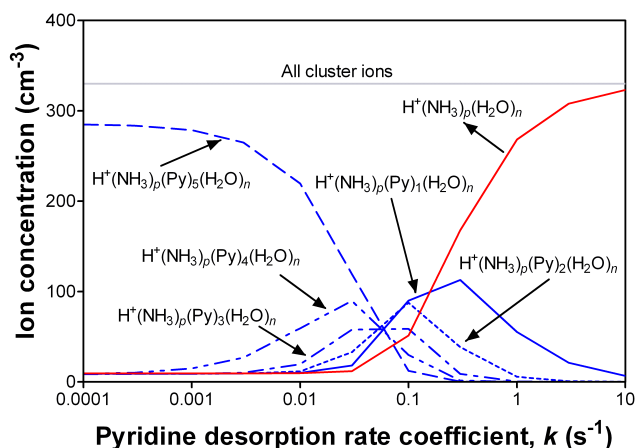


Fig. 9. Concentrations of the most abundant cluster ions as a function of pyridine desorption rate coefficient. The values were calculated using Model B with inclusion of evaporation of pyridine. The initial concentrations are given in Table 2 except the concentration of pyridine that was kept at $9.84 \times 10^7 \text{ cm}^{-3}$.

We also studied the influence of the ammonia concentration on the number of pyridine molecules in the clusters using Model B. Decreasing the ammonia concentration 50 times (shown in Fig. 8c–d) gave no significant change in the concentration of $\text{H}^+(\text{pyridine})_m(\text{H}_2\text{O})_n$ and $\text{H}^+(\text{NH}_3)_p(\text{pyridine})_m(\text{H}_2\text{O})_n$. However, the concentration of $\text{H}^+(\text{CH}_3\text{COCH}_3)_1(\text{H}_2\text{O})_n$ is increased to about 2 cm^{-3} up to a pyridine concentration of about 10^9 cm^{-3} . The concentrations of $\text{H}^+(\text{pyridine})_m(\text{H}_2\text{O})_n$ $1 \leq m \leq 5$ are below 0.1 cm^{-3} except for $\text{H}^+(\text{pyridine})_5(\text{H}_2\text{O})_n$ at pyridine concentrations above $3 \times 10^9 \text{ cm}^{-3}$.

Neglecting evaporation of pyridine from clusters $\text{H}^+(\text{NH}_3)_p(\text{pyridine})_m(\text{H}_2\text{O})_n$ is likely not realistic and we therefore studied the importance of this evaporation using Model B with a pyridine concentration of 4 ppt ($9.9 \times 10^7 \text{ cm}^{-3}$). The evaporation of pyridine was assumed to be proportional to the number of unprotonated pyridine in the cluster. We also assumed that $\text{H}^+(\text{pyridine})_m(\text{H}_2\text{O})_n$ have one protonated pyridine and $\text{H}^+(\text{NH}_3)_p(\text{pyridine})_m(\text{H}_2\text{O})_n$ have none protonated pyridine. The results are shown in Fig. 9. As seen in the figure, a desorption rate coefficient as low as 10^{-3} s^{-1} (3.6 h^{-1}) will influence the cluster distribution. At desorption rate coefficients larger than around 10 s^{-1} , clusters containing pyridine are almost absent.

The above presented results from model calculations are all calculated with an aerosol concentration of 1000 cm^{-3} . In order to study the sensitivity of the cluster ion concentration with respect to the aerosol concentration we performed calculations using Model A with aerosol concentrations varying from 10^2 to 10^4 cm^{-3} and used a fixed pyridine concentration of 4 ppt ($9.9 \times 10^7 \text{ cm}^{-3}$). The results are presented in Figure 10. In clean air (aerosol concentration of 10^2 cm^{-3}) the ion concentrations are slightly higher (around a factor

2) than at intermediate concentrations (aerosol concentration of 10^3 cm^{-3}) but the relation between the cluster ion concentrations are the same. In polluted air (aerosol concentration of 10^4 cm^{-3}) the ion concentration is significantly lower (around a factor 30) than at intermediate concentrations (10^3 cm^{-3}) and the relation between the cluster ion concentrations are also different: the more pyridine molecules in the cluster, the larger the decrease in concentration.

4 Discussion and atmospheric implications

Honma et al. (1992) studied the reaction of $\text{H}^+(\text{H}_2\text{O})_4$ with ND_3 and for all products where the ammonia-d3 molecule entered the cluster all three deuterium atoms remained there after evaporation of H_2O . Effective H/D exchange between molecules in the reaction complex requires a mobile proton (Yamaguchi et al., 2003; Honma and Armentrout 2004; Andersson et al., 2008; Ryding et al., 2011). This observation must be the consequence of strong proton binding most likely due to an adamant NH_4^+ core ion, corresponding to its comparably high pK_a value. It has been shown that this absence of H/D exchange extends to larger sizes (Andersson et al., 2008). Thus we expect protonation exclusively on the ammonia molecule for all clusters formed in the reaction $\text{H}^+(\text{H}_2\text{O})_n + \text{NH}_3 \rightarrow \text{H}^+(\text{NH}_3)_1(\text{H}_2\text{O})_{n-x} + x\text{H}_2\text{O}$. Since the pyridine molecule of a $\text{H}^+(\text{pyridine})_1(\text{H}_2\text{O})_n$ or $\text{H}^+(\text{NH}_3)_1(\text{pyridine})_1(\text{H}_2\text{O})_n$ cluster does not leave after addition of NH_3 , the product will contain two or three basic molecules. This raises a number of interesting questions regarding the cluster structure, dynamics and protonation site. In the case of pure pyridine water clusters, one pyridine molecule in a protonated water cluster leads to locking of the proton (i.e. the proton is bound to the pyridine molecule), while with two or three pyridine molecules in the cluster the proton becomes mobile (Ryding et al., 2011). The situation is more complicated for the present mixed clusters, since we are now dealing with two different types of nitrogen bases. The gas phase proton affinity of pyridine is greater than that of ammonia; they are 930 kJ mol^{-1} and $853.6 \text{ kJ mol}^{-1}$, respectively (Lide, 2006c). However, in bulk water, ammonia is the stronger base as indicated by the higher acid dissociation constant of its conjugate acid ($pK_a = 9.25$ for ammonium, $pK_a = 5.23$ for pyridinium, Lide, 2006a,b). The reversal relation of proton affinities in gas phase and in bulk is presumably a consequence of the ability of ammonium to interact with water through four hydrogen bonds, while pyridinium is limited to one hydrogen bond. Since molecular clusters represent a bridge between the domains of gas phase chemistry and bulk, it is difficult to determine the effective proton affinities, and therefore to which degree the proton will be mobile within the reaction complex. Further studies of clusters containing both ammonia and pyridine using deuterated reactants – for instance D_2O – should provide additional clues.

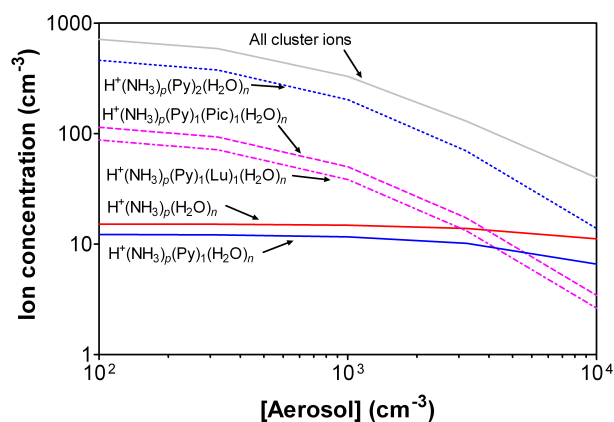


Fig. 10. Concentrations of the most abundant cluster ions as a function of aerosol concentration. The values were calculated using Model A. The initial concentrations are given in Table 2 except the concentration of pyridine that was kept at $9.83 \times 10^7 \text{ cm}^{-3}$ and the aerosol concentration that was varied.

The current setup of the TOF unit does not allow for accurate quantification of product ions below $m/z = 50$. For the $\text{H}^+(\text{H}_2\text{O})_4$ cluster we were only able to measure the reaction products $\text{H}^+(\text{NH}_3)_1(\text{H}_2\text{O})_3$ and $\text{H}^+(\text{NH}_3)_1(\text{H}_2\text{O})_2$ at $m/z = 72$ and $m/z = 54$, respectively. Consequently, the $-3\text{H}_2\text{O}$ peak is missing for this cluster in Fig. 4a. The experiments by Honma et al. (1992) indicate that the reaction leading to formation of $\text{H}^+(\text{NH}_3)_1(\text{H}_2\text{O})_1$ should represent no more than a few percent of the total abundance; the main product is in fact $\text{H}^+(\text{NH}_3)_1(\text{H}_2\text{O})_2$ ($-2\text{H}_2\text{O}$ in Fig. 4a) which constitutes almost the entire reaction cross section, which is in good agreement with the results in Fig. 4a.

For the experimental setup described in Sect. 2.1, applying collision energy in the lab frame below approximately 0.3 eV was observed to result in inefficient ion transmission and major loss of signal. Measurements are possible, although the sampling time would have to be increased many times over. The collision energy used in the measurements, 8 kJ mol^{-1} (COM), was chosen since it allowed for a satisfactory beam intensity to be obtained for all cluster ions studied. This energy is a factor two higher than typical tropospheric collision energies ($\sim 4 \text{ kJ mol}^{-1}$ at room temperature). However, the heating of the formed reaction complex due to addition of NH_3 (i.e. the dissociation energy) is larger still, with values in the range of 65 to 120 kJ mol^{-1} depending on cluster size (based on calculations for clusters with $n = 4$ to 7 using data from Meotner (1984) and Lide (2006c)). The use of higher collision energies would therefore be expected to have only minor effects on the results, as long as the collision energy is sufficiently small compared to the dissociation energy of NH_3 for the cluster in question.

The above mentioned experiment by Honma et al. (1992) show that the total cross section of the $\text{H}^+(\text{H}_2\text{O})_4$ cluster reacting with ND_3 remains virtually unchanged up to collision energies of 20 kJ mol^{-1} (COM). For all measured collision energies in this range, the cross section is made up almost entirely by the reaction forming the product $\text{H}^+(\text{NH}_3)_1(\text{H}_2\text{O})_2$, indicating that the energy released into the cluster upon addition of an ammonia molecule corresponds to evaporation of two H_2O . Based on values calculated using literature thermochemical data (Meotner 1984; Lide 2006c), the energy released by introducing NH_3 into the $\text{H}^+(\text{H}_2\text{O})_4$ cluster is 120 kJ mol^{-1} . The dissociation energies for losing first one H_2O and then a second H_2O from the intermediate cluster $\text{H}^+(\text{NH}_3)_1(\text{H}_2\text{O})_4$ are 44 kJ mol^{-1} and 52 kJ mol^{-1} , respectively. For larger protonated water cluster that reacts with NH_3 at 8 kJ mol^{-1} (COM) we see approximately equal amounts of evaporation of two and three H_2O from the reaction complex (Fig. 4a), implying a somewhat different balance between the dissociation energies of NH_3 and H_2O . As cluster size increases, the energy released into the cluster when NH_3 enters the reaction complex becomes smaller compared to the energy cost of evaporating first one and then a second water molecule. For instance, for $\text{H}^+(\text{H}_2\text{O})_7$, the former is 65 kJ mol^{-1} while the latter two are 35 kJ mol^{-1} and 38 kJ mol^{-1} , respectively. This is contrary to the experimental findings in Fig. 4a. The discrepancy could be due to the fact that the experimental branching ratios do not necessarily represent a sequential loss of H_2O molecules since there is also a possibility of loss of water as a dimer or a trimer (dissociation energies of the dimer and trimer are 20.7 kJ mol^{-1} and 21.7 kJ mol^{-1} , respectively, Santra et al., 2007). Furthermore, the temperature is higher for larger clusters in the beam, which might be part of the explanation. For the pyridine containing clusters in Fig. 4b–c, the tendency is loss of – on average – fewer water molecules post reaction. Even fewer water molecules are lost from the $\text{H}^+(\text{NH}_3)_1(\text{pyridine})_1(\text{H}_2\text{O})_n$ cluster, with the $+\text{NH}_3 - \text{H}_2\text{O}$ and $+\text{NH}_3 - 2\text{H}_2\text{O}$ peaks being of equal size. The latter case is likely to be a consequence of the cluster already containing a NH_3 molecule; a similar effect was observed by Viggiano et al. (Viggiano et al., 1988b) for the cases $\text{H}^+(\text{H}_2\text{O})_n + \text{NH}_3$ and $\text{H}^+(\text{NH}_3)_p(\text{H}_2\text{O})_n + \text{NH}_3$.

Separate measurements of $\text{H}^+(\text{pyridine})_1(\text{H}_2\text{O})_{10}$ and $\text{H}^+(\text{NH}_3)_1(\text{pyridine})_1(\text{H}_2\text{O})_{10}$ reacting with NH_3 at different collision energies give further insights into the impact of E_{COM} on the respective branching ratios. In the case of the former, the branching ratios are essentially unchanged below 8 kJ mol^{-1} , with the branching ratio of $-2\text{H}_2\text{O}$ changing from 0.64 at 8 kJ mol^{-1} to 0.60 at 3 kJ mol^{-1} . The corresponding change for $-\text{H}_2\text{O}$ is from 0.23 to 0.31. For the latter cluster, the changes are somewhat more significant, with both curves having a branching ratio of 0.43 at $E_{\text{COM}} = 8 \text{ kJ mol}^{-1}$. A change in E_{COM} to 3 kJ mol^{-1} results in the $-2\text{H}_2\text{O}$ curve dropping to 0.35 and the $-\text{H}_2\text{O}$ curve increasing to 0.56. It would seem that for this cluster,

the collision energy of choice (8 kJ mol^{-1}) also happens to be the point where the two curves representing the collision energy dependence of the $+\text{NH}_3 - \text{H}_2\text{O}$ product and the $+\text{NH}_3 - 2\text{H}_2\text{O}$ product cross each other. Consequently, for typical tropospheric conditions the $+\text{NH}_3 - \text{H}_2\text{O}$ product would have a higher abundance than the $+\text{NH}_3 - 2\text{H}_2\text{O}$ product for this cluster.

The pure water clusters in Fig. 6 have a somewhat higher reaction rate coefficient for collision with NH_3 compared to the pyridine containing cluster for a large part of the size range. This is very similar to the behaviour exhibited by these three cluster types when reacting with D_2O , as reported in a previous study (Ryding et al., 2011).

Model A gave results that were in excellent agreement with those of Beig and Brasseur (2000) with regards to the concentration of pyridinated cluster ions. Our model is also in agreement with Beig and Brasseur in that the pyridinated cluster ions dominates the tropospheric ion spectrum. Our experiments show that the reaction between $\text{H}^+(\text{pyridine})_1(\text{H}_2\text{O})_n$ and NH_3 does not result in loss of pyridine and that the reaction have a higher rate coefficient than assumed by Beig and Brasseur (by about two orders of magnitude). However, this did not have any significant effect on the modelled cluster distribution. Model A allows for two pyridine derivatives in each cluster ion, and the model calculations show that it should be possible for these clusters to form in the troposphere. In Model B we allowed for up to five pyridines in each cluster ion. The model calculations showed that already at a pyridine concentration of 10^7 cm^{-3} the cluster ion distribution is dominated by clusters containing ammonia, water and five (or more) pyridines (or other amines) when evaporation of pyridine is neglected. When including evaporation of pyridine the outcome depends strongly, as expected, on the evaporation rate coefficient. We estimate that the desorption rate of pyridine was below about 0.1 s^{-1} under the present experimental conditions. As seen in Fig. 9, at this desorption rate the major cluster ions found in Model B are $\text{H}^+(\text{NH}_3)_p(\text{pyridine})_1(\text{H}_2\text{O})_n$ and $\text{H}^+(\text{NH}_3)_p(\text{pyridine})_2(\text{H}_2\text{O})_n$ in equal amounts. However, the temperature of our clusters in the experiments is well below 298 K : hence the evaporation rate of pyridine from water containing clusters at tropospheric temperatures remains unknown.

Measurements by Junninen et al. (2010) and Ehn et al. (2010) suggest that the ions of alkyl substituted pyridine compounds may be more abundant than ordinary protonated pyridine at ground level in urban and boreal environments. This may seem contradictory when considering the atmospheric concentrations of the compounds in question, as well as the lifetime calculations (for instance by Yeung and Elrod, 2003), both of which indicate pyridine as the more common neutral species. However, as pointed out by Junninen et al., the transition from neutral molecule to cation takes place by addition of a proton, which will lead to compounds with higher proton affinity being relatively more abundant in the

tropospheric ion spectrum. The proton affinities in question are 930 kJ mol^{-1} for pyridine, 943.4 to $949.1 \text{ kJ mol}^{-1}$ (depending on isomer) for picoline and 955.4 to $963.0 \text{ kJ mol}^{-1}$ (depending on the isomer) for lutidine (Lide, 2006c). For cluster ions, the type of pyridine or pyridine derivative that enters the clusters (Reactions R1b and R2a) is likely more dependent on concentration than proton affinity. In case of larger water cluster ions with more than one pyridine type molecule the actual protonation site becomes a matter of basicity. Relevant pK_a values are as follows: 5.23 for pyridinium, 5.70 to 6.00 for picolinium (depending on isomer), 6.15 to 6.99 depending on isomer for lutidinium (Lide 2006b). Since the transition from atmospheric pressure to high-vacuum probably leads to a large tendency for fragmentation and/or evaporation of a cluster ion, actual measurements of clusters containing both pyridine and an alkyl substituted variant are likely to be detected as the latter since both the proton affinity and the acid dissociation constants are higher. If also ammonia is present – as indicated by our calculations – the proton may also be situated on the ammonia molecule ($pK_a = 9.25$ for ammonium). The location of the proton is probably also dependent on the cluster size. The fragmentation and evaporation upon sampling could be a reason why clusters containing both ammonia and pyridine (or pyridine derivative) are not observed in the studies by Junninen et al. and Ehn et al. However, our model simulations also show that neglecting evaporation of pyridine in the initial model by Beig and Brasseur may have overestimated the importance of these clusters in the atmosphere. In order to better understand the fragmentation and evaporation processes of these ions during atmospheric measurements, we suggest experimental studies on collision induced dissociation of water cluster ions containing two or more amines. We also suggest detailed studies on evaporation of amines from charged water-containing clusters under tropospheric conditions.

As evident from the measurements by Ehn et al. many ions are missing in order for our model to be universal. Including all ions today is not realistic since many reactions with these ions have unknown rate coefficients. We regard pyridine in our model to represent most amines in the atmosphere and our model should therefore be a good simplification of the complex cluster ion reactions taking place in the troposphere. However, we emphasise that there is a great need for new laboratory measurements and innovative field measurements to determine reaction- and desorption rate coefficients in order to improve the model and our understanding of cluster ion formation in the troposphere. For instance, during field measurements of air ions we suggest that the concentrations of neutral amines are also measured.

Supplementary material related to this article is available online at:

<http://www.atmos-chem-phys.net/12/2809/2012/acp-12-2809-2012-supplement.zip>.

Acknowledgements. This work was supported by the Swedish Research Council, the Norwegian Research Council by the Grant No. 179568/V30 to the Centre for Theoretical and Computational Chemistry through their Centre of Excellence program, and the Nanoparticle in Interactive Environments platform at the Faculty of Science at University of Gothenburg. MJR is grateful for travel grants awarded by the University of Gothenburg through Jubileumsfonden and Filosofiska fakultetens gemensamma donationsnämnd.

Edited by: M. Kulmala

References

- Andersson, P. U., Ryding, M. J., Sekiguchi, O. and Uggerud, E.: Isotope exchange and structural rearrangements in reactions between size-selected ionic water clusters, $\text{H}_3\text{O}^+(\text{H}_2\text{O})_n$ and $\text{NH}_4^+(\text{H}_2\text{O})_n$, and D_2O , *Phys. Chem. Chem. Phys.*, 10, 6127–6134, 2008.
- Arijs, E. and Brasseur, G.: Acetonitrile in the Stratosphere and Implications for Positive-Ion Composition, *J. Geophys. Res. Atmos.*, 91, 4003–4016, 1986.
- Atkinson, R., Tuazon, E. C., Wallington, T. J., Aschmann, S. M., Arey, J., Winer, A. M. and Pitts, J. N.: Atmospheric Chemistry of Aniline, N,N-Dimethylaniline, Pyridine, 1,3,5-Triazine, and Nitrobenzene, *Environ. Sci. Technol.*, 21, 64–72, 1987.
- Beig, G.: Global change induced trends in ion composition of the troposphere to the lower thermosphere, *Ann. Geophys.*, 26, 1181–1187, 2008, <http://www.ann-geophys.net/26/1181/2008/>.
- Beig, G. and Brasseur, G. P.: Model of tropospheric ion composition: A first attempt, *J. Geophys. Res. Atmos.*, 105, 22671–22684, 2000.
- Beig, G., Walters, S. and Brasseur, G.: A 2-Dimensional Model of Ion Composition in the Stratosphere .1. Positive-Ions, *J. Geophys. Res. Atmos.*, 98, 12767–12773, 1993.
- Clemo, G. R.: Some Aromatic Basic Constituents of Coal Soot, *Tetrahedron*, 29, 3987–3990, 1973.
- Ehn, M., Junninen, H., Petäjä, T., Kurtén, T., Kerminen, V.-M., Schobesberger, S., Manninen, H. E., Ortega, I. K., Vehkamäki, H., Kulmala, M., and Worsnop, D. R.: Composition and temporal behavior of ambient ions in the boreal forest, *Atmos. Chem. Phys.*, 10, 8513–8530, doi:10.5194/acp-10-8513-2010, 2010.
- Eisele, F. L.: Direct Tropospheric Ion Sampling and Mass Identification, *Int. J. Mass Spectrom. Ion Processes*, 54, 119–126, 1983.
- Eisele, F. L.: Identification of Tropospheric Ions, *J. Geophys. Res. Atmos.*, 91, 7897–7906, 1986.
- Eisele, F. L.: First tandem mass spectrometric measurement of tropospheric ions, *J. Geophys. Res. Atmos.*, 93, 716–24, 1988.
- Eisele, F. L. and McDaniel, E. W.: Mass-Spectrometric Study of Tropospheric Ions in The Northeastern and Southwestern United-States, *J. Geophys. Res. Atmos.*, 91, 5183–5188, 1986.
- Eisele, F. L. and Tanner, D. J.: Identification of ions in continental air, *J. Geophys. Res. Atmos.*, 95, 20539–50, 1990.
- FACSIMILE v4.0 User Guide: MCPA Software Ltd, Oxford, UK, 2007.
- Hauck, G. and Arnold, F.: Improved Positive-Ion Composition Measurements in the Upper Troposphere and Lower Stratosphere and the Detection of Acetone, *Nature*, 311, 547–550, 1984.
- Honma, K. and Armentrout, P. B.: The mechanism of proton exchange: Guided ion beam studies of the reactions, $\text{H}(\text{H}_2\text{O})_n^+(n=1-4)+\text{D}_2\text{O}$ and $\text{D}(\text{D}_2\text{O})_n^+(n=1-4)+\text{H}_2\text{O}$, *J. Chem. Phys.*, 121, 8307–8320, 2004.
- Honma, K., Sunderlin, L. S. and Armentrout, P. B.: Reactions of Protonated Water Clusters with Deuterated Ammonia – $\text{H}(\text{H}_2\text{O})_N^+(N=1-4) + \text{ND}_3$, *Int. J. Mass Spectrom. Ion Processes*, 117, 237–259, 1992.
- Horrak, U., Salm, J., and Tammet, H.: Statistical characterization of air ion mobility spectra at Tahkuse Observatory: Classification of air ions, *J. Geophys. Res.-Atmos.*, 105, 9291–9302, 2000.
- Junninen, H., Ehn, M., Petäjä, T., Luosujärvi, L., Kotiaho, T., Koskiainen, R., Rohner, U., Gonin, M., Fuhrer, K., Kulmala, M., and Worsnop, D. R.: A high-resolution mass spectrometer to measure atmospheric ion composition, *Atmos. Meas. Tech.*, 3, 1039–1053, doi:10.5194/amt-3-1039-2010, 2010.
- Lide, D. R.: Dissociation Constants of Inorganic Acids and Bases, CRC Handbook of Chemistry and physics, internet version 2006, D. R. Lide. Boca Raton, FL, USA, Taylor and Francis, 2006a.
- Lide, D. R.: Dissociation Constants of Organic Acids and Bases, CRC Handbook of Chemistry and physics, internet version 2006, D. R. Lide. Boca Raton, FL, USA, Taylor and Francis, 2006b.
- Lide, D. R.: Proton Affinities, CRC Handbook of Chemistry and physics, internet version 2006, D. R. Lide. Boca Raton, FL, USA, Taylor and Francis, 2006c.
- Meotner, M.: The Ionic Hydrogen-Bond and Ion Solvation 2. Solvation of Onium Ions by One to 7 H_2O Molecules – Relations between Monomolecular, Specific, and Bulk Hydration, *J. Am. Chem. Soc.*, 106, 1265–1272, 1984.
- Perkins, M. D. and Eisele, F. L.: First mass-spectrometric measurements of atmospheric ions at ground level, *J. Geophys. Res. Atmos.*, 89, 9649–57, 1984.
- Ryding, M. J., Zatul, A. S., Andersson, P. U. and Uggerud, E.: Isotope exchange in reactions between D_2O and size-selected ionic water clusters containing pyridine, $\text{H}+(\text{pyridine})_m(\text{H}_2\text{O})_n$, *Phys. Chem. Chem. Phys.*, 13, 1356–1367, 2011.
- Saintjalm, Y. and Morettesta, P.: Study of Nitrogen-Containing Compounds in Cigarette-Smoke by Gas Chromatography-Mass Spectrometry, *J. Chromatogr.*, 198, 188–192, 1980.
- Santra, B., Michaelides, A. and Scheffler, M.: On the accuracy of density-functional theory exchange-correlation functionals for H bonds in small water clusters: Benchmarks approaching the complete basis set limit, *J. Chem. Phys.*, 127, 2007.
- Schlager, H., Fabian, R., and Arnold, F.: A new cluster ion source/ion drift cell apparatus for atmospheric ion studies – First mobility and reaction rate coefficient measurements, 3rd Int. Swarm Seminar, Innsbruck, Austria, 1983.
- Schulte, P. and Arnold, F.: Pyridinium Ions and Pyridine in the Free Troposphere, *Geophys. Res. Lett.*, 17, 1077–1080, 1990.
- Tanner, D. J. and Eisele, F. L.: Ions in Oceanic and Continental Air Masses, *J. Geophys. Res. Atmos.*, 96, 1023–1031, 1991.
- Vana, M., Ehn, M., Petaja, T., Vuollekoski, H., Aalto, P., de Leeuw,

- G., Ceburnis, D., O'Dowd, C. D. and Kulmala, M.: Characteristic features of air ions at Mace Head on the west coast of Ireland, *Atmos. Res.*, 90, 278–286, 2008.
- Wayne, R. P.: *Chemistry of Atmospheres*, Oxford, Oxford University Press, 2000.
- Viggiano, A. A., Dale, F., and Paulson, J. F.: Proton transfer reactions of aquated hydrogen ions ($H+(H_2O)_n$, $n=2-11$) with methanol, ammonia, pyridine, acetonitrile, and acetone, *J. Chem. Phys.*, 88, 2469–77, 1988a.
- Viggiano, A. A., Morris, R. A., Dale, F., and Paulson, J. F.: Tropospheric Reactions of $H+(NH_3)_M(H_2O)_N$ with Pyridine and Picoline, *J. Geophys. Res. Atmos.*, 93, 9534–9538, 1988b.
- Yamaguchi, S., Kudoh, S., Okada, Y., Orii, T., Takeuchi, K., Ichikawa, T., and Nakai, H.: Size-dependent reaction cross section of protonated water clusters $H+(H_2O)_n$ ($N=2-11$) with D_2O , *J. Phys. Chem. A*, 107, 10904–10910, 2003.
- Yeung, L. Y. and Elrod, M. J.: Experimental and computational study of the kinetics of OH plus pyridine and its methyl- and ethyl-substituted derivatives, *J. Phys. Chem. A*, 107, 4470–4477, 2003.
- Yu, F. Q.: Nucleation rate of particles in the lower atmosphere: Estimated time needed to reach pseudo-steady state and sensitivity to H_2SO_4 gas concentration, *Geophys. Res. Lett.*, 30, 1526–1529, 2003.
- Yu, F. Q. and Turco, R. P.: Ultrafine aerosol formation via ion-mediated nucleation, *Geophys. Res. Lett.*, 27, 883–886, 2000.
- Zhao, Z., Huskey, D. T., Olsen, K. J., Nicovich, J. M., McKee, M. L., and Wine, P. H.: Kinetics, mechanism, and thermochemistry of the gas-phase reaction of atomic chlorine with pyridine, *Phys. Chem. Chem. Phys.*, 9, 4383–4394, 2007.